

Predicting the Merger Fraction of Lyman alpha Emitters from Redshift $z \sim 3$ to $z \sim 7$

V. Tilvi^{1*}, E. Scannapieco¹, S. Malhotra¹, and J. E. Rhoads¹

¹*School of Earth and Space Exploration, Arizona State University, Tempe, AZ 85287, USA.*

24 February 2024

ABSTRACT

Rapid mass assembly, likely from mergers or smooth accretion, has been predicted to play a vital role in star-formation in high-redshift Ly α emitters. Here we predict the major merger, minor merger, and smooth accreting Ly α emitter fraction from $z \approx 3$ to $z \approx 7$ using a large dark matter simulation, and a simple physical model that is successful in reproducing many observations over this large redshift range. The central tenet of this model, different from many of the earlier models, is that the star-formation in Ly α emitters is proportional to the mass accretion rate rather than the total halo mass. We find that at $z \approx 3$, nearly 35% of the Ly α emitters accrete their mass through major (3:1) mergers, and this fraction increases to about 50% at $z \approx 7$. This implies that the star-formation in a large fraction of high-redshift Ly α emitters is driven by mergers. While there is discrepancy between the model predictions and observed merger fractions, some of this difference ($\sim 15\%$) can be attributed to the mass-ratio used to define a merger in the simulation. We predict that future, deeper observations which use a 3:1 definition of major mergers will find $\geq 30\%$ major merger fraction of Ly α emitters at redshifts ≥ 3 .

Key words: cosmology – theory: dark matter, galaxies–high-redshift: interactions: halos, methods: numerical

1 INTRODUCTION

While several theoretical models of Ly α emitters have been developed (e.g. Barton et al. 2004; Davé et al. 2006; Tasitsiomi 2006; Shimizu et al. 2007; Nagamine et al. 2008; Le Delliou et al. 2006; Kobayashi et al. 2007, 2009; Dayal et al. 2008; Samui et al. 2009) we still lack a complete understanding of how mass assembly and star-formation occurs in these galaxies. It is likely that mergers are the dominant mode of mass accretion resulting in star-formation in at least some fraction ($\geq 20\%$) of Ly α emitters (e.g. Pirzkal et al. 2007; Bond et al. 2009; Taniguchi et al. 2009).

Recently, Tilvi et al. (2009) developed a physical model of Ly α emitters which is successful in explaining many observable including number density, stellar mass, star-formation rate, and clustering properties of Ly α emitters from $z \approx 3$ to $z \approx 7$. This model differs fundamentally from many of the earlier models (e.g. Haiman & Spaans 1999; Dijkstra et al. 2007; Mao et al. 2007; Stark et al. 2007; Fernandez & Komatsu 2008) in that the star-formation of Ly α emitters, and hence their Ly α luminosity is proportional to the mass accretion rate rather than the total halo mass.

In this paper, we combine the above model with a large dark matter cosmological simulation to predict the major merger, minor merger, and smooth accreting Ly α emitter fraction from $z \approx 3$ to $z \approx 7$. We also carefully assess the uncertainties in our model predictions. We note that currently there are no theoretical prediction of merger fraction of Ly α emitters.

On the observational front, only recently it has been possible to estimate the merger fraction of Ly α emitters. At $z \sim 0.3$, Cowie et al. (2010) found that $\geq 30\%$ of Ly α emitters are either irregulars or have disturbed morphologies indicative of mergers. At higher redshifts, $z > 3$, the observed merger fraction varies from $\approx 20\%$ to $\approx 45\%$ (Pirzkal et al. 2007; Bond et al. 2009; Taniguchi et al. 2009).

Recently, Cooke et al. (2010) found that all Lyman-break galaxies (LBGs) that have close companions ($\leq 15h^{-1}$ Mpc) exhibit strong Ly α emission lines. In the spectroscopically confirmed close pairs, the spectra/imaging show double Ly α emission peak/double morphology confirming that these LBGs at $z \approx 3$ are indeed mergers. Cooke et al. (2010) also studied a sample of spectroscopically confirmed LBGs at $z \approx 3$ from Shapley et al. (2006), and found that about 33% of LBGs with strong Ly α emission have double Ly α emission peaks, strengthening the above conclusion.

The outline of this paper is as follows. In §2 we briefly

* E-mail: tilvi@asu.edu

describe the physical model of Ly α emitters (Tilvi et al. 2009), our simulations, and how we construct the merger trees. In §3, we estimate the merger fraction of Ly α emitters, discuss the effect of mass resolution in the simulation on our results, and compare our model predictions with the observations. In §4 we quantify the uncertainties associated with the predictions, and we summarize our results in §5.

2 METHODS

2.1 Modeling Ly α Emitters

Our method is based on carrying out dark matter (DM) only simulations, and then populating the halos from these simulations with Ly α emitters according to a simple physical model presented in Tilvi et al. (2009). This model uses a single parameter to successfully reproducing many observed properties of Ly α emitters, including their luminosity functions, stellar masses, stellar ages, star formation rates, and clustering from $z = 3.1$ to $z = 6.6$. The central tenet of this model is that the Ly α luminosity is proportional to the star formation rate *i.e.*

$$L_{\text{Ly}\alpha} = 1 \times 10^{42} \times \frac{\text{SFR}}{\text{M}_{\odot} \text{yr}^{-1}} \text{ erg s}^{-1}, \quad (1)$$

which in turn is proportional to the mass accretion rate *i.e.* $\text{SFR} = f_{\star} \times \dot{M}_b$. Here, f_{\star} and \dot{M}_b are the star formation efficiency (*i.e.* converting baryonic mass to stars), and the baryonic mass accretion rate. As we use DM only simulations, the baryonic mass accretion rate is obtained by converting DM mass accretion assuming universal ratio of baryonic to DM densities. For more details about this model, we refer the reader to Tilvi et al. (2009).

2.2 Simulation and Halo Catalogs

In order to implement this method, we carried out a large N-body DM cosmological simulation (hereafter Gadget-1024), with the GADGET2 (Springel 2005) code. We generated the initial conditions for the simulation using second-order Lagrangian Perturbation Theory (Crocce et al. 2006; Thacker & Couchman 2006). In this simulation we use 1024^3 DM particles, each particle with a mass $M_p \approx 2.7 \times 10^7 \text{ M}_{\odot} h^{-1}$ evolved in a comoving volume of $(102 \text{ Mpc})^3$. Using a Friends-of-Friends (FOF) halo finder (Davis et al. 1985), we identify DM halos that contain 100 or more DM particles. This corresponds to a minimum halo mass $M_{\text{halo}} \approx 2.7 \times 10^9 \text{ M}_{\odot} h^{-1}$.

We then generate catalogs, for redshifts from $z = 10$ to $z = 3$, which contain positions of halos, their DM mass, and unique IDs of each individual particle that belongs to a given halo. These unique particle IDs are later used to track halos between two epochs. Throughout this chapter we assumed a flat Λ CDM cosmology with parameters $\Omega_m = 0.233$, $\Omega_{\Lambda} = 0.721$, $\Omega_b = 0.0462$, $h = 0.71$, $\sigma_8 = 0.817$ where Ω_m , Ω_{Λ} , Ω_b , h , and σ_8 correspond, respectively, to the matter density, dark energy density, and baryonic density in units of the critical density, the Hubble parameter in units of $100 \text{ km s}^{-1} \text{ Mpc}^{-1}$, and the RMS density fluctuations on the $8 \text{ Mpc } h^{-1}$ scale, in agreement with WMAP (Spergel et al. 2007) five year results (Hinshaw et al. 2009).

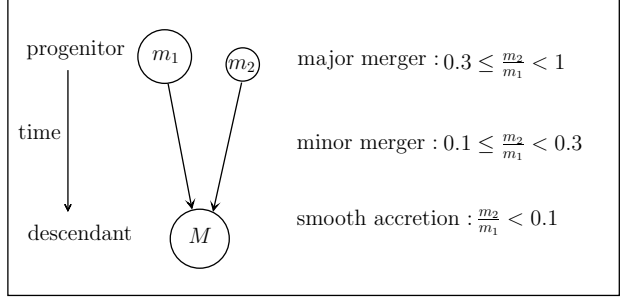


Figure 1. Merger schematic showing classification of mergers based on the progenitor mass ratio.

2.3 Ly α Emitter Catalogs

To construct a simulated population of Ly α emitters, we first calculate the amount of DM mass that is accreted by each halo in time $t_{\text{Ly}\alpha} = 30 \text{ Myr}$ (Tilvi et al. 2009). This time interval was chosen so as to match with the average stellar population of Ly α emitters. This mass accretion rate is then converted to the Ly α luminosity as described in Section 2.1. While, in general, we expect every halo to accrete more mass with time, we find that some halos lose mass (negative accretion) which is due to the limitation of halo-finding technique. We correct for this simulation noise by counting the number of halos that have negative mass accretion in each mass bin and subtracting this from corresponding counts in the positive mass bins (See Tilvi et al. (2009) for more details). With this procedure we now have Ly α emitter catalogs from $z = 6.6$ to $z = 3$.

It is possible that the mass resolution in our simulation might affect our results. In order to carefully assess this effect, we also used the Millenium-II simulation (Boylan-Kolchin et al. 2009) which has a larger volume, and a higher halo mass resolution. In particular, it follows 2160^3 particles with each particle having a DM mass $6.885 \times 10^6 \text{ M}_{\odot} h^{-1}$ in a simulation volume of $(141 \text{ Mpc})^3$. Furthermore, in this simulation, each halo is identified by a unique ID allowing us to follow the same procedure as applied to our Gadget-1024 simulation. We use Millenium-II simulation only to investigate the simulation mass resolution effect since the time step between each output is about ten times larger, making it unsuitable for our final comparisons with observations.

2.4 Merger Tree

As described in Section 2.1, each Ly α emitter is assigned a luminosity based on its mass accretion rate. This mass accretion can occur when either two or more *progenitors* (halos at time step $S-1$) merge into a single *descendant* (halo at a later time step S), or when a single progenitor evolves into a single descendant (see Figure 1).

We then classify each merger into one of three categories: major merger, minor merger, or smooth accretion, based on the progenitor mass ratio. In particular, we define each of these cases as:

- (1) major merger: $0.3 \leq m_2/m_1 \leq 1$,
- (2) minor merger: $0.1 \leq m_2/m_1 < 0.3$, and
- (3) smooth accretion: $m_2/m_1 < 0.1$,

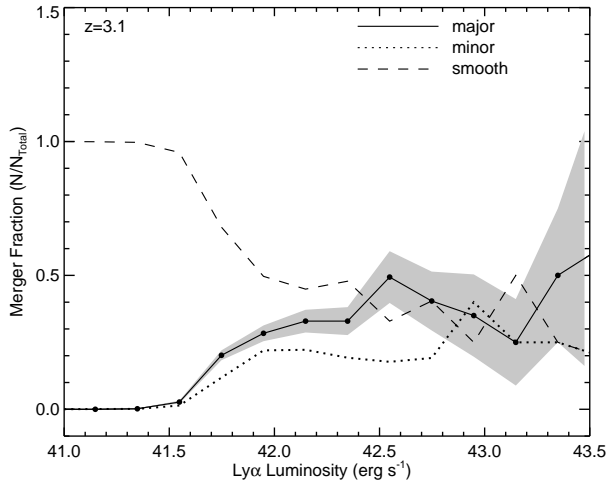


Figure 2. The fraction of $\text{Ly}\alpha$ emitters that have formed from major mergers, minor mergers, and smooth accretion at $z = 3.1$. The major and minor merger fractions are shown in solid, and dotted lines respectively, while the long dashed line shows the fraction of $\text{Ly}\alpha$ emitters that accrete mass through smooth accretion. The shaded area are the poisson errors on the major merger fraction. About 35% of the $\text{Ly}\alpha$ emitters at $z \approx 3$ accrete their mass through major mergers. The steep decline in the major merger fraction at $\text{Log Ly}\alpha < 42 \text{ erg s}^{-1}$ is not real but results from limited simulation mass resolution (see Section 3).

where m_1 and m_2 are the masses of the most massive, and second-most massive progenitors associated with a single descendant (see Figure 1). In the case where a descendant halo has a single progenitor halo, by default, this halo is assigned a smooth accretion mode. Using the above criteria we now have a merger tree, *i.e.* each descendant halo, and hence each $\text{Ly}\alpha$ emitter, has been associated with the mode of mass accretion *i.e.* major merger, minor merger or smooth accretion.

3 MODEL RESULTS AND OBSERVATIONAL COMPARISONS

3.1 Merger Fraction at $z \approx 3$

Using this method we are able to calculate the fraction of $\text{Ly}\alpha$ emitters that have undergone major mergers, minor mergers, and smooth accretion. Here, we remind the reader that each descendant halo hosts one $\text{Ly}\alpha$ emitter. In effect, every descendant halo is an $\text{Ly}\alpha$ emitter with its luminosity proportional to the mass accretion rate. We define the merger fraction as the ratio of number of $\text{Ly}\alpha$ emitters formed from mergers in a given luminosity bin to the total number of $\text{Ly}\alpha$ emitters in that bin. Thus,

$$f(L) = \frac{N_m(L)}{N_T(L)}, \quad (2)$$

where $N_m(L)$ is the number of $\text{Ly}\alpha$ emitters formed from mergers, and $N_T(L)$ is the total number of $\text{Ly}\alpha$ emitters in that luminosity bin.

Figure 2 shows the merger fractions of $\text{Ly}\alpha$ emitters that have formed from major mergers, minor mergers, and smooth accretion, at $z = 3.1$. The major merger, and minor

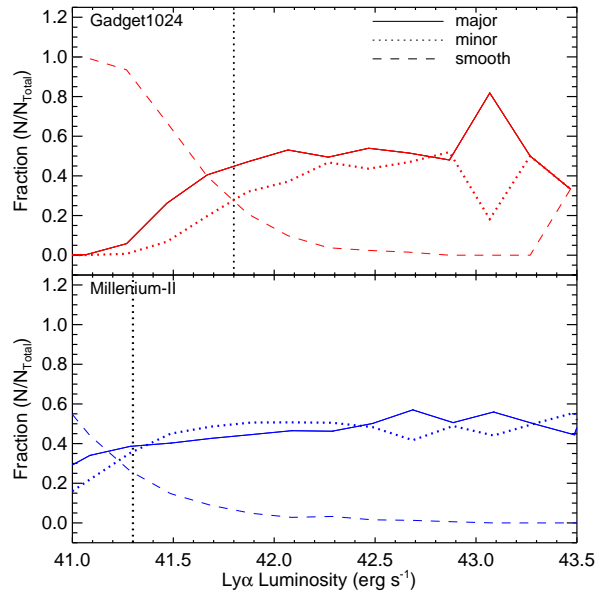


Figure 3. Comparing the merger fractions between Gadget1024 and the Millenium-II simulation. The vertical dotted lines represent the luminosity range below which our results are not reliable. In the Millenium-II simulation, due to higher mass resolution, the vertical dotted line shift towards the lower luminosity. Also seen is the decreased noise at the brighter luminosities in the Millenium-II simulation due to its larger simulation volume.

merger fractions are shown in solid and dotted lines respectively, while the long dashed line indicates the fraction of $\text{Ly}\alpha$ emitters formed from smooth accretion. The shaded region shows the Poisson errors on the major merger fraction.

From Figure 2 it is evident that at $z = 3.1$, about 35% of $\text{Ly}\alpha$ emitters are formed from major mergers. In other words the dominant mode of mass accretion, and hence star-formation in nearly 35% of $\text{Log}(\text{Ly}\alpha) > 42 \text{ erg s}^{-1}$ emitters, occurs through major mergers, while remaining 65% of $\text{Ly}\alpha$ emitters accrete their mass through minor mergers and smooth accretion combined.

Note that the Poisson errors dominate the bright end of the $\text{Ly}\alpha$ luminosity. Our results might not be fully reliable below $6 \times 10^{41} \text{ erg s}^{-1}$ where we see a steep decline in the major merger fraction. This effect might be partly due to lower halo mass resolution. To understand and quantify this effect of lower halo mass resolution, we now compare our results from figure 2 with the Millenium-II simulation which has about 2.6 times more volume, and nearly forty times better mass resolution. In addition, we also investigate the effect of stellar ages ($t_{\text{Ly}\alpha}$) of $\text{Ly}\alpha$ emitters on our predictions.

3.2 Effect of Halo Mass Resolution and $t_{\text{Ly}\alpha}$

Using the same procedure as described in Section 2, we constructed a $\text{Ly}\alpha$ emitter catalog from the Millenium-II simulation, at a common redshift, $z = 6.8$ between the two simulations. In Figure 3 we compare the results from the two simulations. The top panel are the results from our Gadget-1024 simulation while the bottom panel shows the merger fraction obtained from Millenium-II simulation. The

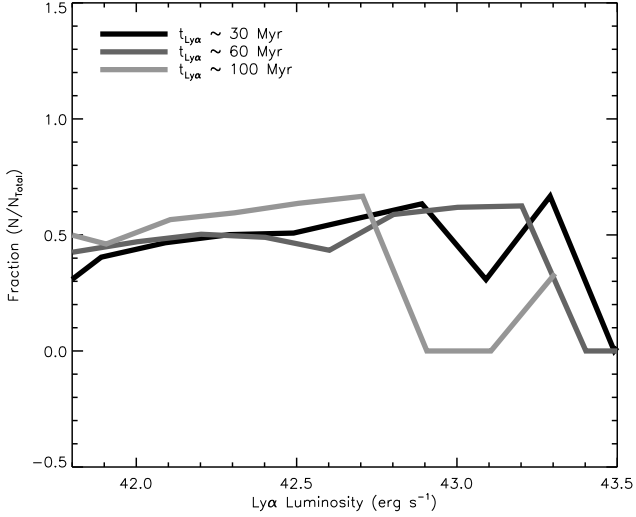


Figure 4. Model prediction of major merger fraction for different stellar ages of $\text{Ly}\alpha$ emitters at $z \approx 7$. The smaller $t_{\text{Ly}\alpha}$ implies younger stellar population in $\text{Ly}\alpha$ emitters.

vertical dotted lines show the luminosity below which the apparent decline in the major merger fraction is caused due to lower halo mass resolution. This luminosity range shift towards lower $\text{Ly}\alpha$ luminosity in the Millennium-II simulation (lower panel) which has a better mass resolution. Also, at the bright end of the luminosity axis, the fluctuation in the merger fraction is lesser in the Millennium-II simulation due to the larger volume. Thus, better mass resolution is needed to estimate the merger fractions reliably at lower luminosities, and a larger simulation volume to minimize the noise at the brighter luminosities. Hereafter, in our analysis, we consider only those $\text{Ly}\alpha$ emitters that have $\text{Ly}\alpha$ luminosity $> 6 \times 10^{41} \text{ erg s}^{-1}$.

We now study the effect of $t_{\text{Ly}\alpha}$ on our model predicted results. For our model $\text{Ly}\alpha$ emitters the luminosity is proportional to the mass accretion rate ($\Delta M_b / t_{\text{Ly}\alpha}$) where we assumed a fixed $t_{\text{Ly}\alpha} = 30 \text{ Myr}$ which corresponds to the average stellar ages of $\text{Ly}\alpha$ emitters. While this is true for average population, from observations it is inferred that this stellar age ranges from 1 Myr to even hundred Myr (e.g. Finkelstein et al. 2007).

Figure 4 shows the major merger fractions of our model $\text{Ly}\alpha$ emitters at $z = 6.6$ for $t_{\text{Ly}\alpha} = 30, 60$, and 100 Myr . While the stellar ages have changed by a factor of 3, we find no or little change in major merger fraction. Thus, our model predictions are independent of the stellar ages of $\text{Ly}\alpha$ emitters.

3.3 Redshift Evolution of Merger Fraction

In preceding sections we have shown that the predicted merger fractions are affected by the mass resolution, and that there is no dependence of $t_{\text{Ly}\alpha}$ on the predicted merger fractions. We now investigate the redshift evolution of merger fraction of $\text{Ly}\alpha$ emitters.

Figure 5 shows the redshift evolution of major merger fraction (left panel), minor merger fraction (middle panel), and smooth accretion (right panel) from $z = 3.1$ to $z = 6.6$.

The major merger fraction (left panel), and smooth accretion (right panel) show a mild evolution with redshift. On the other hand, the minor merger fraction is nearly constant. At $z = 3.1$ the average major merger fraction $f_{\text{major}} \approx 35\%$. Similarly, the average fraction of minor mergers (middle panel) and smooth accretion (right panel) are $f_{\text{minor}} \approx 25\%$, and $f_{\text{smooth}} \approx 40\%$ respectively. At $z = 6.6$, the major merger fraction is higher with $f_{\text{major}} \approx 50\%$. Thus, at higher redshifts, the mass accretion and hence the star-formation in a significant fraction of the $\text{Ly}\alpha$ emitters occurs through major and minor mergers.

3.4 Comparison with the Observations

In this section we compare only major merger fractions with the observations since it is extremely difficult to identify minor mergers from observations especially at higher redshifts.

Only recently, has it been possible to estimate the observed merger fraction of $\text{Ly}\alpha$ emitters at high-redshifts. For example, at $z = 5.7$ Taniguchi et al. (2009) have studied morphological properties of $\text{Ly}\alpha$ emitters in the COSMOS field using HST/ACS. Only two out of about 50 $\text{Ly}\alpha$ emitters show clear signs of extended features, an indication of either interacting or merging galaxies. However, there is a large uncertainty in estimating merger fraction from these observations due to their shallow survey depth.

In Figure 6, we compare this result with our model predictions. The downward arrow indicates the upper limit on the merger fraction at $z = 5.7$. At this redshift, our model predicted major merger fraction is about 50%. While comparing our model predictions with the observations we have accounted for the observed limiting $\text{Ly}\alpha$ luminosity at corresponding redshifts.

At slightly lower redshift $z \approx 5$, (Pirzkal et al. 2007) studied morphologies of nine $\text{Ly}\alpha$ emitters in HUDF. To quantify the morphologies, they used *concentration*(C), and *asymmetry*(A) parameters (Conselice et al. 2000) and found that nearly 44% have clumpy or complex structures. Visually, about 33% sources look morphologically disturbed or as ongoing mergers, while nearly 10% of the sources can not be reliably identified as mergers. This observed merger fraction is nearly same as our model prediction.

Bond et al. (2009) studied morphological properties of about 120 $z \sim 3.1$ $\text{Ly}\alpha$ emitting galaxies in the rest-frame ultra-violet band. They found that at least 17% of the total $\text{Ly}\alpha$ emitters contain multiple components which might indicate that these are either individual star-forming regions within a single galaxy, a merged system or ongoing mergers. Since it is very difficult, due to their compact sizes (e.g. Malhotra et al 2011, Bond et al 2011), to definitely conclude whether the multi-component $\text{Ly}\alpha$ emitters are the remnants of mergers or if these are individual star-forming regions in a single system, we have shown the merger fraction by upward and downward arrows indicating uncertainties in both directions. Their classification is based on counting the number of components in a fixed aperture. At $z = 3.1$, our model predicted major merger fraction is about 35%, much higher than the observed fraction. However, in Section 4 we show that, some of this difference between model predictions and observations can be attributed to the definition of major merger mass ratio.

At lower redshift, $z \approx 0.3$, Cowie et al. (2010) stud-

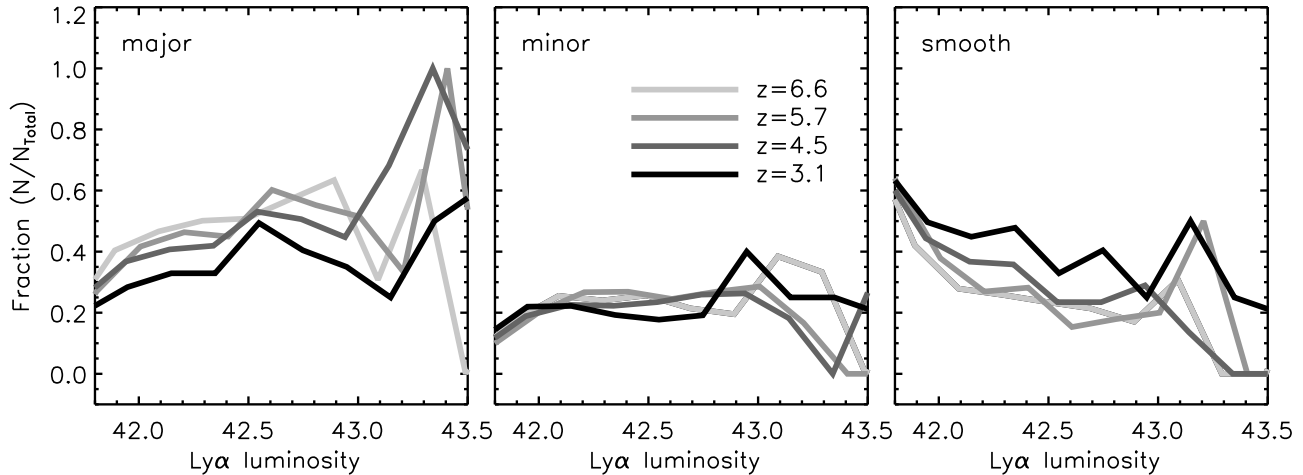


Figure 5. Redshift evolution of major merger fraction (left panel), minor merger fraction (middle), and smooth accretion (right panel) from $z = 3.1$ to $z = 6.6$. We see a mild evolution of major merger fraction (left), and in smooth accretion (right). On the other hand the minor merger fraction remains constant over this redshift range.

ied morphologies of Ly α emitters in the GROTH00 and SIRTFFL00 fields. They found that $> 30\%$ of the Ly α emitters show signs of ongoing mergers. Based on the above comparisons, there is some discrepancy between our model prediction and observations. In the following section, we investigate the uncertainty due to the mass ratio used to define a merger.

4 UNCERTAINTIES FROM MODEL PREDICTIONS AND OBSERVATIONS

4.1 Dependence of Merger Fraction on the Progenitor Mass Ratio Definition

We now vary the progenitor mass ratio criteria from 1:3 to 1:2, *i.e.* major mergers are now defined as those for which $0.5 \leq m_2/m_1 \leq 1$, while for $0.1 \leq m_2/m_1 < 0.5$, they are classified as minor mergers. All other Ly α emitters with their progenitor halo mass ratio $m_2/m_1 < 0.1$ are defined as smooth accreting. In figure 7 (see also Figure 2) we show the predicted merger fraction dependence on the progenitor mass ratio definition.

By changing the progenitor mass ratio from 1:3 to 1:2, the major (minor) merger fraction drops (increases) by about 15%. Thus, it is clear that the predicted merger fraction of Ly α emitters depends on the progenitor mass ratio definition, and one needs to be careful when comparing model predicted merger fractions with the observations since the merger defining mass ratio influences the merger fractions.

4.2 Merger Observability Timescale

In addition to the above uncertainty, the observed merger fraction depends on the timescale, t_{obs} (observability timescale) during which a merger can be identified as a merger. For example, if t_{obs} is shorter than $t_{Ly\alpha}$, the time during which a galaxy is observed as an Ly α emitter, then the observed merger fraction will be underestimated.

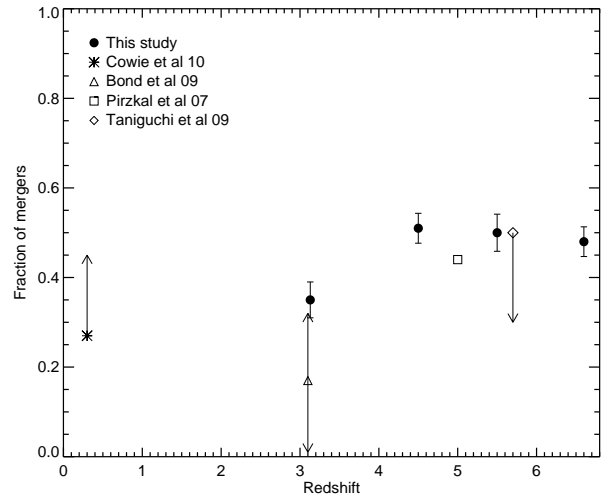


Figure 6. Comparison of our model predicted major merger fraction with the observations. Filled circles are our model prediction while other symbols represent observations at $z = 5.7$ (Taniguchi et al 2009), $z \approx 5$ (Pirzkal et al. 2007), $z = 3.1$ (Bond et al. 2009), and $z \approx 0.3$ (Cowie et al. 2010). Error bars on model predictions indicate Poisson errors.

According to our model (see equation 1), merging of two galaxies results in an Ly α emitter with its Ly α luminosity proportional to the mass accretion rate. If, say two galaxies merge on a dynamical timescale (t_{dyn}), then it will be observed as a merger for a period $t_{dyn} = t_{obs}$.

Using $t_{dyn} = \sqrt{3\pi/(16G\rho(z))}$, where $\rho(z)$ is the average overdensity of the collapsing object, we find that at $z \approx 3$, $t_{dyn} \approx 300$ Myr, much larger than $t_{Ly\alpha} = 30$ Myr. Thus, we expect to miss no or little merger fraction of Ly α emitters at $z \geq 3$, due to the observability timescale. The dynamical time, however is nearly half with $t_{dyn} \approx 130$ Myr at $z \approx 6$.

As can be seen from the above discussion that while the predicted merger fraction is not affected by the merger ob-

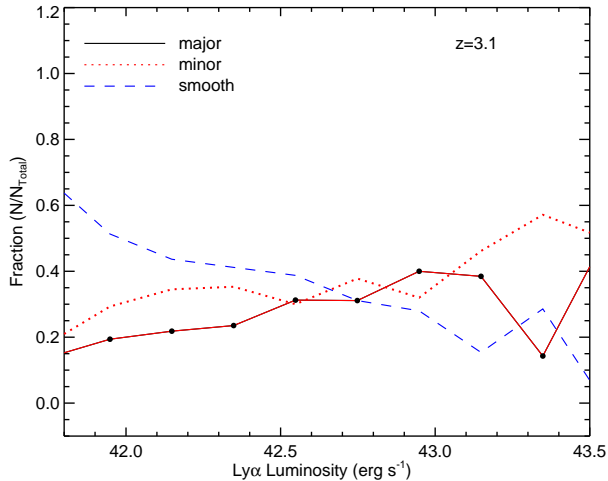


Figure 7. Progenitor mass ratio dependence on the predicted merger fraction of $\text{Ly}\alpha$ emitters at $z = 3.1$. Here, the major merger is defined as $0.5 \leq m_2/m_1 \leq 1$, while for the minor merger $0.1 \leq m_2/m_1 < 0.5$. All $\text{Ly}\alpha$ emitters with its progenitor mass ratio $m_2/m_1 < 0.1$ are defined as smooth accreting.

servability timescale, there is some uncertainty in the predicted merger fraction due to the defining mass ratio. In addition, a large uncertainty is due to the shallower survey depths especially at higher-redshifts.

5 SUMMARY AND CONCLUSIONS

Motivated by our earlier work (Tilvi et al. 2009) based on a simple physical model of $\text{Ly}\alpha$ emitters, combined with a large dark matter cosmological simulation, we have predicted the major merger, minor merger, and smooth accreting $\text{Ly}\alpha$ emitter fraction from $z \approx 3$ to $z \approx 7$. The model presented in Tilvi et al. (2009), different from many of the earlier models in that the star-formation rate is proportional to the mass accretion rate rather than the total halo mass, has been successful in reproducing many observed physical properties including the luminosity functions, stellar ages, star formation rates, stellar masses, and clustering properties of $\text{Ly}\alpha$ emitters from $z \approx 3$ to $z \approx 7$.

We carefully constructed the merger tree from $z \approx 7$ to $z \approx 3$, accounting for the uncertainties in the halo finder. In this merger tree, each descendent halo was associated with its progenitor(s), and based on the progenitor mass ratio, each merger was classified as either major, minor merger or smooth accretion. We also carefully assessed how our predicted results might be affected by several parameters including halo mass resolution, defining merger mass ratio, stellar ages of $\text{Ly}\alpha$ emitters, and the merger observability timescale. We summarize our key results below:

- At $z \approx 3$, about 35% of $\text{Ly}\alpha$ emitters accrete their mass through major mergers, and this fraction increases to about 50% at redshift $z \approx 7$. On the other hand, at this redshift, the minor mergers and smooth accretion contribute equally in the remaining 50% of the $\text{Ly}\alpha$ emitters. Thus, at higher redshifts, mergers play an important role in mass

assembly and hence the star-formation in majority of the $\text{Ly}\alpha$ emitters.

- We also compared our model predicted major merger fraction with the observations and found that our model over-predicts the major merger fraction. This discrepancy can be resolved if we take into account the uncertainties in defining the merger classification mass ratio. By changing the major merger mass ratio from 3:1 to 2:1, we found that the predicted major merger fraction decreases by about 15%. We predict that future, deeper imaging surveys and using spectroscopic methods such as the one demonstrated in Cooke et al. (2010), should find $\geq 30\%$ merger fraction of $\text{Ly}\alpha$ emitters at high-redshifts.

This work was supported in part by the grant HST-0808165. All simulations were performed on the *saguaro* cluster operated by the Fulton School of Engineering at Arizona State University.

REFERENCES

- Barton, E. J., Davé, R., Smith, J.-D. T., Papovich, C., Hernquist, L., & Springel, V. 2004, *ApJL*, 604, L1
- Bond, N. A., Gawiser, E., Gronwall, C., Ciardullo, R., Altmann, M., & Schawinski, K. 2009, *ApJ*, 705, 639
- Bond, N., Gawiser, E., Guaita, L., et al. 2011, *arXiv:1104.2880*
- Boylan-Kolchin, M., Springel, V., White, S. D. M., Jenkins, A., & Lemson, G. 2009, *MNRAS*, 398, 1150
- Conselice, C. J., Bershadsky, M. A., & Gallagher, J. S., III 2000, *AAP*, 354, L21
- Cooke, J., Berrier, J. C., Barton, E. J., Bullock, J. S., & Wolfe, A. M. 2010, *MNRAS*, 403, 1020
- Cowie, L. L., Barger, A. J., & Hu, E. M. 2010, *ApJ*, 711, 928
- Crocce, M., Pueblas, S., & Scoccimarro, R. 2006, *MNRAS*, 373, 369
- Davé, R., Finlator, K., & Oppenheimer, B. D. 2006, *MNRAS*, 370, 273
- Davis, M., Efstathiou, G., Frenk, C. S., & White, S. D. M. 1985, *ApJ*, 292, 371
- Dayal, P., Ferrara, A., & Gallerani, S. 2008, *MNRAS*, 389, 1683
- Dijkstra, M., Wyithe, J. S. B., Haiman, Z. 2007, *MNRAS*, 379, 253D
- Fernandez, E. R., & Komatsu, E. 2008, *MNRAS*, 384, 1363
- Finkelstein, S. L., Rhoads, J. E., Malhotra, S., Pirzkal, N., & Wang, J. 2007, *ApJ*, 660, 1023
- Haiman, Z., & Spaans, M. 1999, *ApJ*, 518, 138
- Hinshaw, G., et al. 2009, *ApJS*, 180, 225
- Kobayashi, M. A. R., Totani, T., & Nagashima, M. 2007, *ApJ*, 670, 919
- Kobayashi, M. A. R., Totani, T., & Nagashima, M. 2009, *arXiv:0902.2882*
- Le Delliou, M., Lacey, C. G., Baugh, C. M., & Morris, S. L. 2006, *MNRAS*, 365, 712
- Malhotra, S., Rhoads, J. E., Finkelstein, S. L., et al. 2011, *arXiv:1106.2816*
- Mao, J., Lapi, A., Granato, G. L., de Zotti, G., & Danese, L. 2007, *ApJ*, 667, 655
- Nagamine, K., Ouchi, M., Springel, V., & Hernquist, L. 2008, *arXiv:0802.0228*

- Pirzkal, N., Malhotra, S., Rhoads, J. E., & Xu, C. 2007, ApJ, 667, 49
- Samui, S. et al. 2009
- Shapley, A. E., Steidel, C. C., Pettini, M., Adelberger, K. L., & Erb, D. K. 2006, ApJ, 651, 688
- Shimizu, I., Umemura, M., & Yonehara, A. 2007, MNRAS, 380, L49
- Spergel, D. N., et al. 2007, ApJS, 170, 377
- Springel, V. 2005, MNRAS, 364, 1105
- Stark, D. P., Loeb, A., & Ellis, R. S. 2007, ApJ, 668, 627
- Taniguchi, Y., et al. 2009, ApJ, 701, 915
- Tasitsiomi, A. 2006, ApJ, 645, 792
- Thacker, R. J. & Couchman, H. M. P., 2006, Int. J. High Perf. Comp. & Net., 4, 303
- Tilvi, V., Malhotra, S., Rhoads, J. E., Scannapieco, E., Thacker, R. J., Iliev, I. T., & Mellema, G. 2009, ApJ, 704, 724